SUPPLEMENTAL APPENDIX

SUPPLEMENTAL ACKNOWLEDGMENTS

We are grateful to Bloomington Stock Center (NIH P40OD018537) for providing the fly strains used in this study and Mar Ruiz Gomez, Centro de Bio-logia Molecular, Madrid, for the nephrocyte heat fixation protocol. This work was performed under the Care4Rare Canada Consortium funded by Genome Canada, the Canadian Institutes of Health Research, the Ontario Genomics Institute, Ontario Research Fund, Genome Quebec and Children's Hospital of Eastern Ontario Research Foundation. Steering committee members and their affiliations of Care4Rare Canada are

Kym Boycott[44], Alex MacKenzie[44], Michael Brudno[45,46], Dennis Bulman[44] & David Dyment[44]

[44]Children's Hospital of Eastern Ontario Research Institute, University of Ottawa, 401 Smyth Road, Ottawa, Ontario, Canada K1H 8L1.
[45]Department of Computer Science, University of Toronto, Ontario, Canada.
[46]Donnelly Centre and Banting and Best Department of Medical Research, University of Toronto, Toronto, Ontario, Canada.

SUPPLEMENTALTABLES AND FIGURES

Supplemental Table 1. Target sequences of siRNAs used in this study.

Human *SGPL1*	
siRNA#5	CAUCAUUGGUGUUGUAUAG
siRNA#6	GAAACGAGUAGCUAUACAA
siRNA#7	CAUUAUUGGUCGUAAGAUU
siRNA#8	GAACGGCUAUGUUGAAGCU
Rat *Sgpl1*	
siRNA#9	CUAAAGGAUAUCCGGGAAU
siRNA#10	AGUUUAUGGUCUCGGUUUA
siRNA#11	GCUCUGGGCUCCAACCGAUU
siRNA#12	GAAUGAAGAUUGUACGCGU

Supplemental Table 2. *Drosophila Sply* locus cloning and mutagenesis primers.

Sply* locus cloning	
Sply Forward 1	TGATCTGGTGGAGCTCGTCACT
Sply Reverse 1	AACCGCTCCACCTTCGCTCA
Sply Forward *2*	GATTTGGCAGCAAGTGTTGGT
Sply Reverse *2*	GAAATCCCTGTACGCCTTCA
Mutagenesis primers	
Sply HA tag Forward	CACTCCCAGCCAGAAATACCCATACGATGTTCCCGATTACGCTTAGACAC CTGGAGC
Sply HA tag Reverse	GCTCCAGGTGTCTAAGCGTAATCGGGAACATCGTATGGGTATTTCTGGCT GGGAGTG
Sply E119G Forward	CCTCCGACTGGTAGATGGGCACCTGAAGACTGG
Sply E119G Reverse	CCAGTCTTCAGGTGCCCATCTACCAGTCGGAGG
Sply R210Q Forward	CCATGAAGGCATACCAGGATTTCGCTAGAGAG
Sply R210Q Reverse	CTCTCTAGCGAAATCCTGGTATGCCTTCATGG
Sply S335I Forward	GGTTAAGGGTGTGACCATTATCTCCGCTGATACC
Sply S335I Reverse	GGTATCAGCGGAGATAATGGTCACACCCTTAACC

* *Sply* locus cloning was performed by amplifying two partially overlapping regions followed by homologous recombination.

Supplemental Table 3. Immunological profile of patient EB-1.

Comprehensive analysis of leukocyte subpopulations by multi-color flow cytometry was performed using the following 4 HIPC panels: T-cell-panel: CD45; CD3; CD4; CD8; CD28; CD38; CD45RA; CD57; CD127; CD183; CD185; CD196; CD197; CD278; CD279; HLA-DR; TCR×™; Treg-panel: CD45; CD25; CD4; CCR4; CD127; CD45R0; CD3; HLA-DR; B-cell-panel: CD10; CD45; CD24; CD19; IgD; CD38; CD20; CD27; CD3; Innate-panel: CD45; CD56; CD123; CD11c; CD16; CD3+CD19+CD20 (dump); CD14; HLA-DR.11 Briefly 100 µl of whole blood was added to the panel tubes with pre-mixed antibodies and incubated for 30 minutes at room temperature in the dark with light agitation. After red cell lysis, cells were fixed and analyzed on a BD Fortessa instrument. A complete and detailed protocol for HIPC immunophenotyping can be downloaded from www.entire-net.eu /sops-and-cats.

Patient EB-1 suffered from severe lymphopenia (218/µl $CD4^+$; 23/µl $CD8^+$; 25/µl γ/δ T cells and 39/µl B cells). Among the $CD4^+$-lymphocytes only 19% of the cells displayed a naïve phenotype, T_{EM} represented 42%, T_{CM} 23% and T_{EMRA} 16% of the cells. In the $CD8^+$- compartment 47% of the cells showed a naïve phenotype, T_{EM} represented 27% and T_{EMRA} 22% of the cells. The few circulating B cells also showed mostly a memory phenotype. Remarkably 36% of the circulating B cells were plasmablasts. The number of regulatory T cells was in the normal range, the same for NK cells, however the proportion of $CD56^{br}CD16^+$ was elevated. Monocytes were in the normal range, the ratio of myeloid to plasmacytoid DC's was 2:1. Functional analysis was performed using gene expression analysis after whole blood LPS and PMA/ionomycin stimulation. After LPS stimulation the expression of pro-inflammatory genes was decreased in comparison to the reference group. After P/I stimulation the expression of most cytokines was decreased, perhaps due to the low T cell count. The expression of TNFSF13B (BAFF) was elevated both spontaneously and after stimulation.

Flow-cytometry

T cells				B cells	NK cells	Monocytes	Dendritic cells
CD4+	**CD8+**	**γδ T cells**	**Treg**				
218/µL ⇓⇓⇓⇓ (1400-5200/µl) Naïve: 19%# T_{EM}: 42% T_{CM}: 23% T_{EMRA}: 16%	23/µL ⇓⇓⇓⇓ (600-3000/µl) Naïve:47%# T_{EM}: 27% T_{EMRA}: 22%	25/µl (17-221/µl)*	65/µl (56-104/µl)*	39/µl ⇓⇓⇓⇓ (500-3600/µl) 72% memory cells## 36% plasmablasts	376/µl (200-1800/µl)	725/µl (700-1500/µl)	228/µl (29-156/µl)* Myeloid to plasmacytoid DC ratio 2:1 (6:1)*

Functional analysis

	Spontaneous		LPS		PMA/Ionomycin	
	EB-1	**Reference**	**EB-1**	**Reference**	**EB-1**	**Reference**
IFNgamma	2**	9 ± 15	8	122 ± 142	7014	122576 ± 50241
IL1ß	486	2035 ± 1885	5481	26377 ± 8366	2438	3694 ± 1616
IL2	3	1 ± 1	12	1 ± 1	5649	103217 ± 43349
IL4	4	4 ± 3	0	8 ± 4	412	2101 ± 1143
IL6	2	9 ± 9	590	6568 ± 4057	72	423 ± 270
IL8	4832	6921 ± 6511	9939	20984 ± 11090	364760	75382 ± 53044
IL10	2	3 ± 1	12	13 ± 7	21	1046 ± 645
IL12-p40	0	0 ± 0	0	141 ± 142	1	0 ± 0
IL17	0	0 ± 0	0	0 ± 0	42	3526 ± 1496
IL22	0	0 ± 0	0	1 ± 1	64	4143 ± 2068
TNFalpha	27	175 ± 172	92	965 ± 686	627	6573 ± 4669
TNFSF13B	1681	260 ± 152	1607	544 ± 408	482	38 ± 37

T EM- Effector memory T cells; TCM- Central memory TEMRA- Effector memory RA T cells; *range not age-matched; # naive T cells constitute usually >80% of the T cells in this age group; ## memory B cells constitute usually <6% of the B cells in this age group **Transcripts / 1000 transcripts PPIB

SUPPLEMENTAL FIGURES

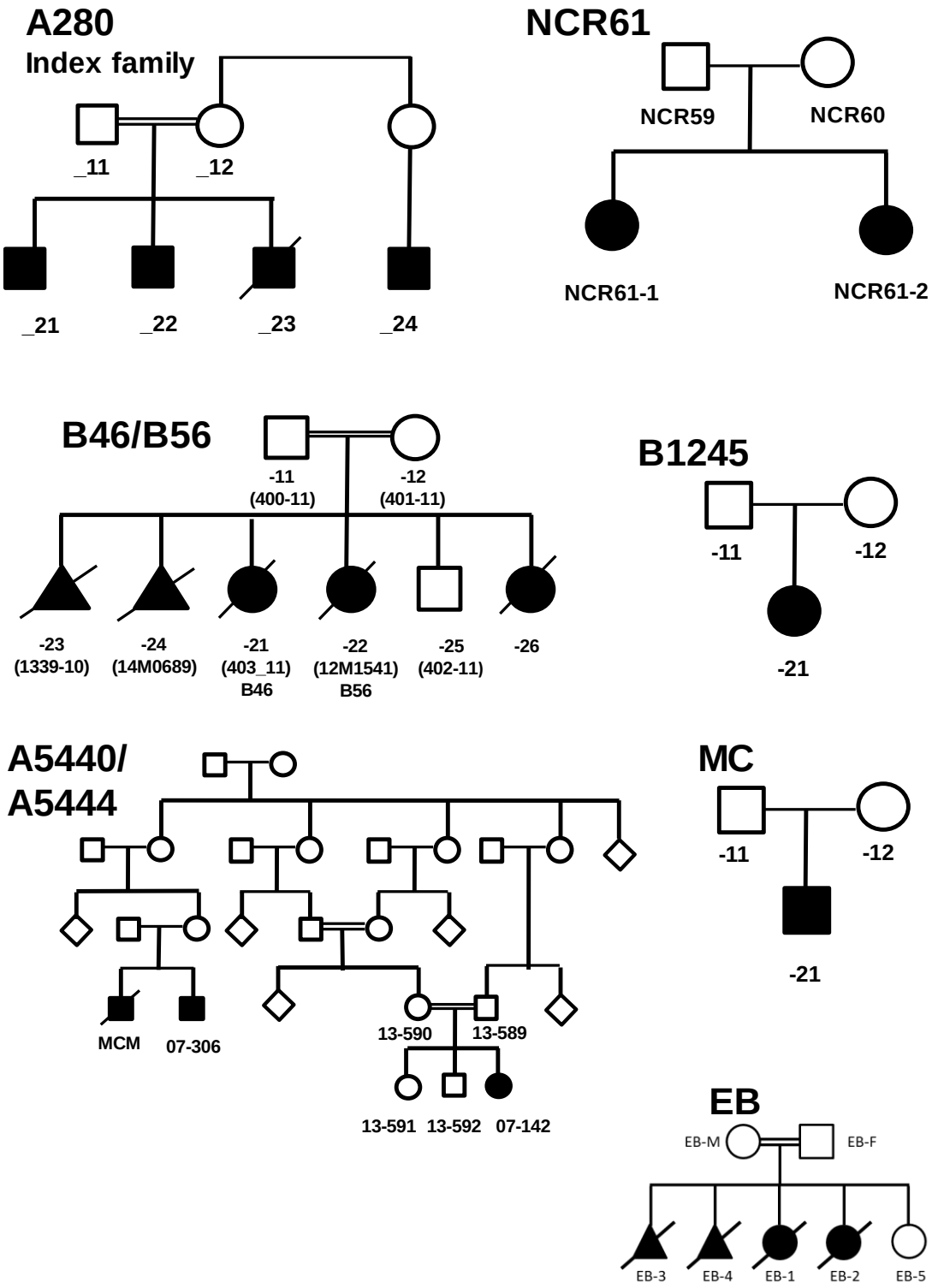

Supplemental Figure 1. Pedigrees of 7 families with *SGPL1* mutations.
Pedigrees of Family A280, NCR 61, B46/B56, A5440/A54444, MC, EB and B1245 are shown. Squares indicate male family members, circles female family members, triangles unknown gender, slashes deceased individuals, solid symbols affected family members and double horizontal bars consanguinity. Numbers below circles and squares indicate the sibling number. Symbols without numbers indicates that DNA was not available for these individuals.

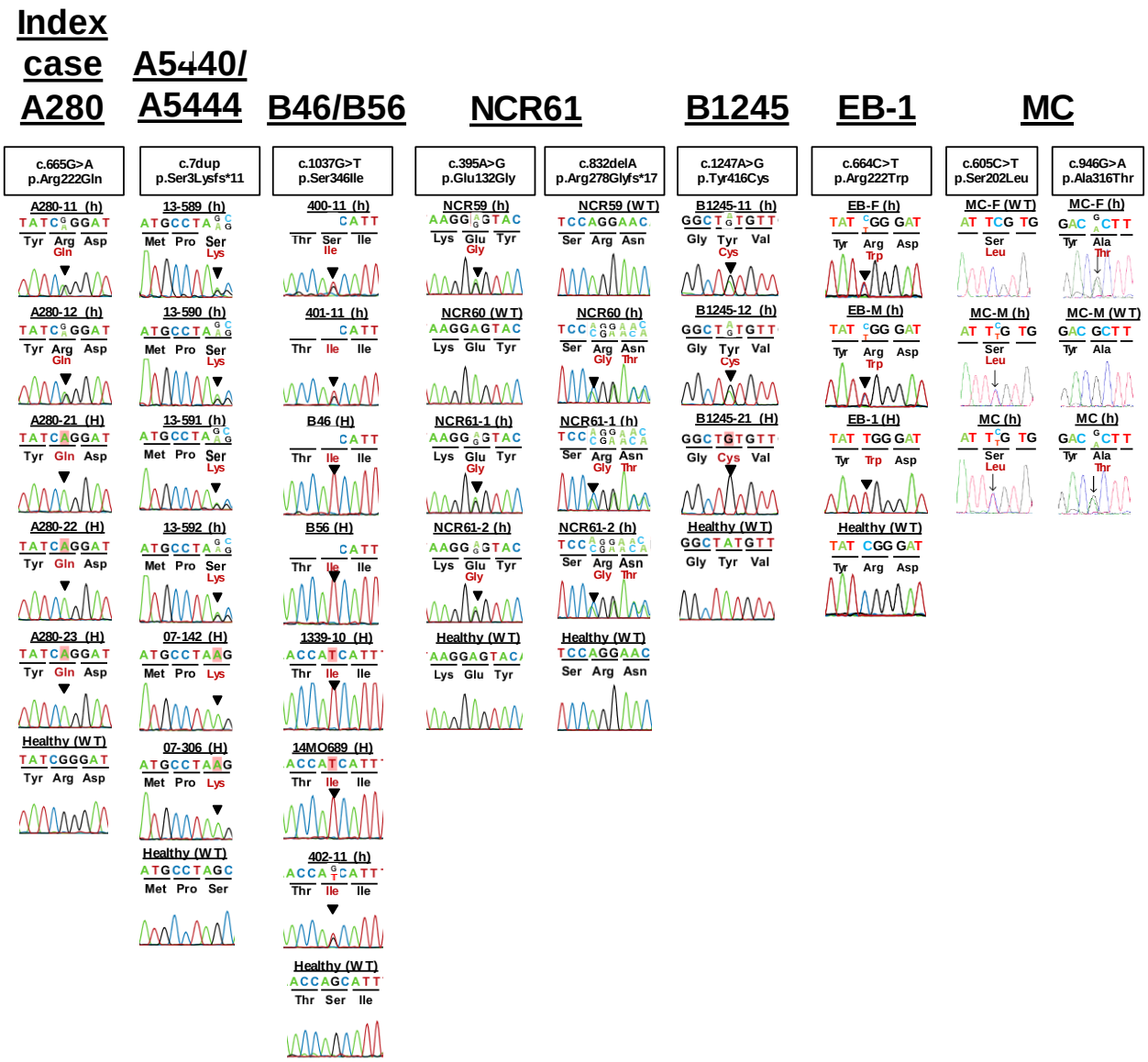

Supplemental Figure. 2. Sequencing traces of individuals with mutation in *SGPL1*.
Sequencing traces are shown for individuals from 5 families with mutations in *SGPL1* for families A280, A5440/A5444, B46/B56, NCR61, B1245, EB and MC. Arrowheads denote altered nucelotides.

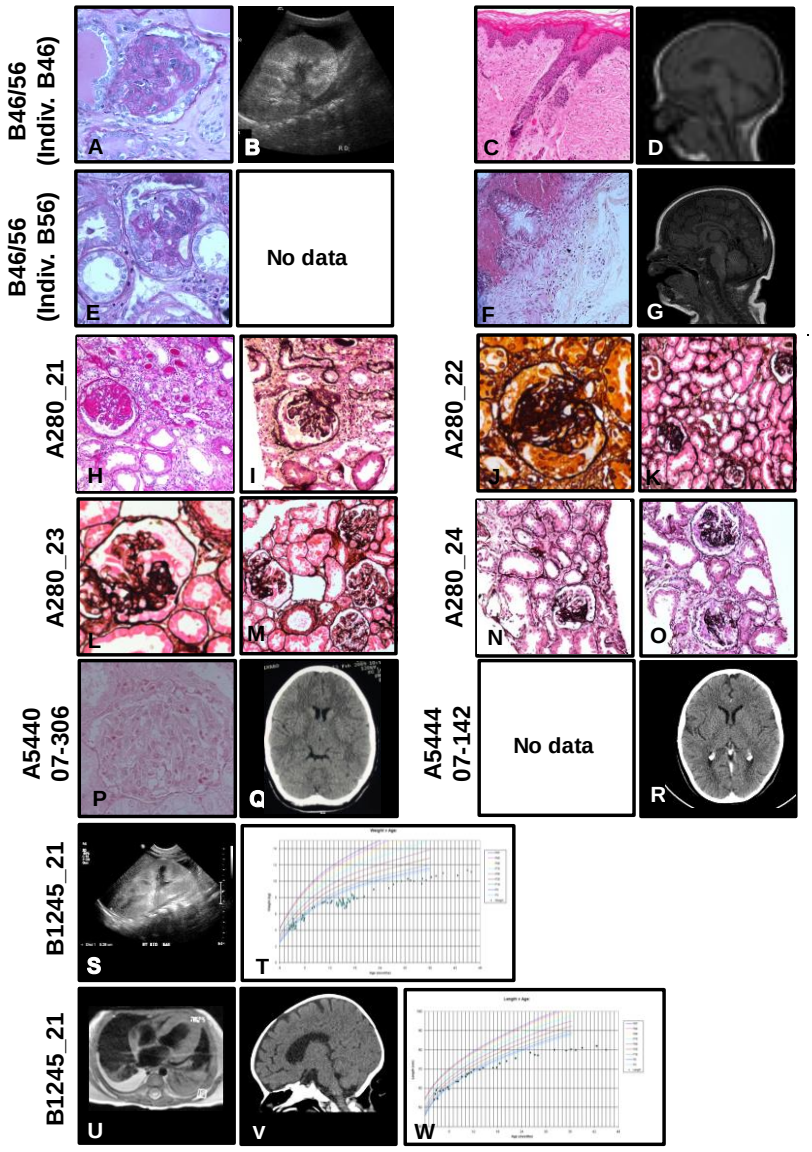

Supplemental Figure 3. Additional clinical phenotypes of individuals with mutations in *SGPL1*. Family and individual numbers are shown per row. **(A)** Renal histology in individual B46 showing diffuse mesangial sclerosis (DMS). **(B)** Renal ultrasound in B46. **(C)** Skin biopsy in B46 showing a moderate degree of hyperkeratosis with a reduced and focally absent granular layer. Infundibula of hair follicles are dilated with keratotic follicular plugs. The dermis and cell-rich stroma are normal. No signs of inflammation, or vacuolar/granular degeneration of keratinocytes. Image is considered characteristic for ichthyosis vulgaris. **(D)** Cranial MRI of B46 showing microcephaly. **(E)** Renal histology of B56 showing DMS. **(F)** Skin biopsy of B56 showing ichthyosis vulgaris. **(G)** Cranial MRI of B56 showing microcephaly. **(H, I)** Renal histology of A280_21 showing global sclerosis and focal segmental glomerulosclerosis (FSGS). (J, K) Renal histology of A280_22 with FSGS (silver methenamine staining). **(L, M)** Renal histology of A280_23 with limited tubular atrophy, expanded mesangium and global and segmental glomerulosclerosis. **(N, O)** Renal histology of A280_24 showing FSGS. **(P)** Renal histology images of A5440/07-306 individual with mutations in SGPL1 showing focal-segmental glomerular sclerosis. **(Q)** Brain CT scan in individual A5440/07-306, microcephaly is not present **(R)** Brain CT scan in individual A5444/07-142, microcephaly is not present. **(S)** Renal sonography in individual B1245_21. **(T)** Body weight percentiles for B1245_21 with failure to thrive. **(U)** Cardiac MR of B1245_21 with reduced left ventricular systolic function (EF~50%) and reduced diastolic function. **(V)** Brain CT scan of B1245_21. Microcephaly is not present. **(W)** Height percentiles for B1245_21 with failure to thrive with height <3rd%.

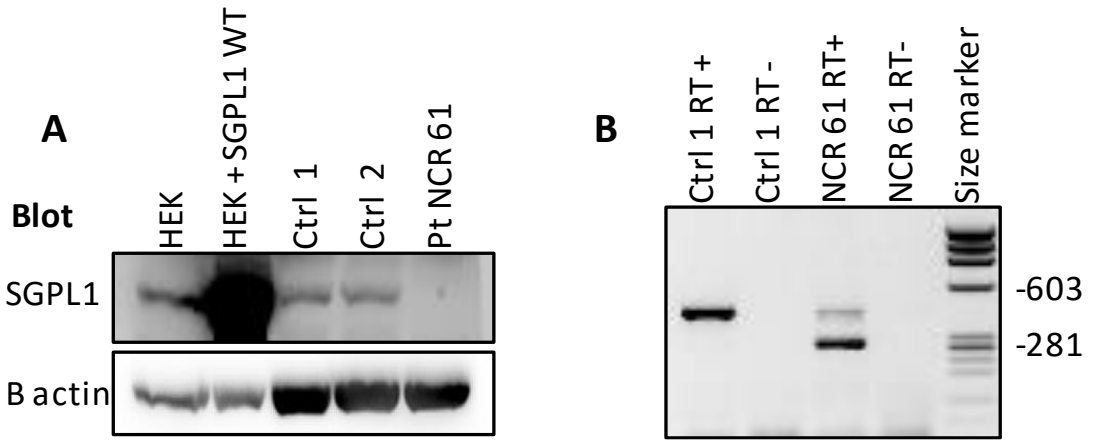

Supplemental Figure 4. Immunoblot in patient fibroblasts and consequence of *SGPL1* splice site mutation c.395A>G.

(A) SGPL1 protein is absent from NCR61 patient fibroblasts. While SGPL1 is present in control fibroblasts it is absent from patient NCR61. HEK 293 cells were transfected with SGPL1 WT as a control for SGPL1 antibody. n=3 independent experiments

(B) SGPL1 shows splicing defects in NCR61 patient fibroblasts. Reverse transcriptase of mRNA from control and patient NCR61 fibroblasts was performed, followed by PCR amplification of SGPL1 exon 4 to 8, cloning of the amplicons and sequencing. Note the amplification of a light band at the expected size that corresponds to the frameshift allele (c.832delA) and a lower size amplicon corresponding to the loss of exon 5 due to the c.395A>G mutation from the other allele. Sequencing of the c.395A>G product revealed the resulting truncating allele p.Ile88Thrfs*25.

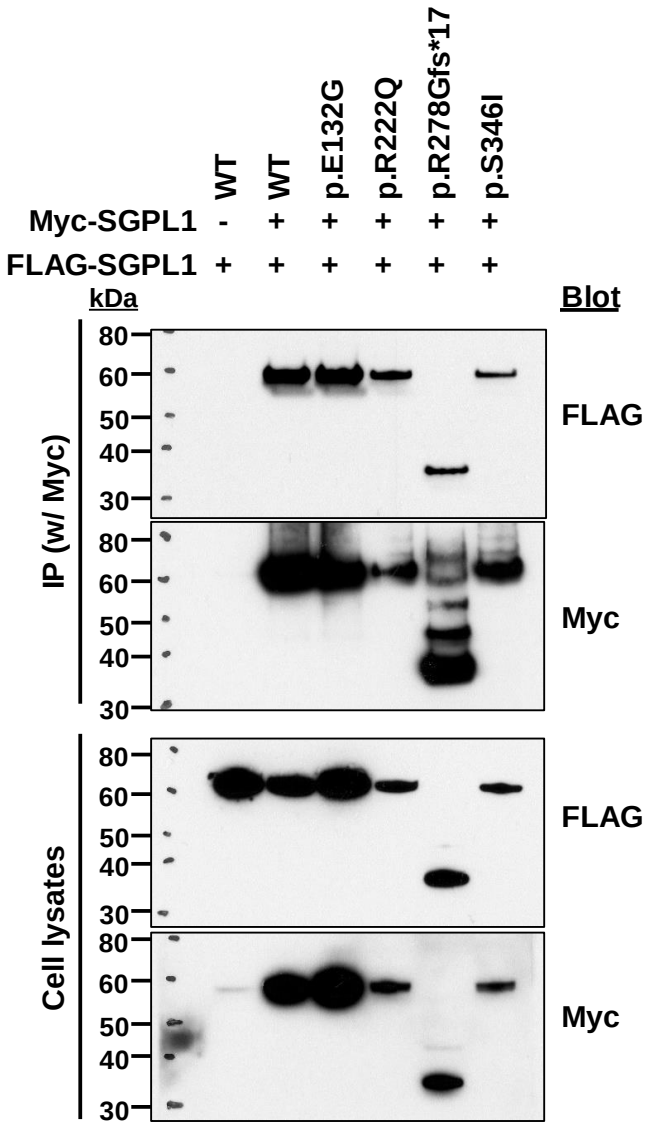

Supplemental Figure 5. Co-immunoprecipitation to assess dimerization of wild type (WT) and mutant SGPL1 protein. Reciprocal experiment to **Figure 2I**. HEK293T cells were transfected with Myc- and FLAG-tagged SGPL1 WT and mutant plasmids. Cell lysates were coimmunoprecipitated with anti-Myc antibody and blotted with anti-FLAG antibody to examine the dimers of WT or mutant SGPL1 proteins. Note that, while all proteins, including the truncated protein (p.Arg278Glyfs*17), still form dimers, p.Arg222Gln and p.Ser346Ile mutant proteins exhibit lower expression levels compared to WT protein upon overexpression in HEK293T cells (see **also Figure 2I**). Coimmunoprecipitation is representative of 3 experiments.

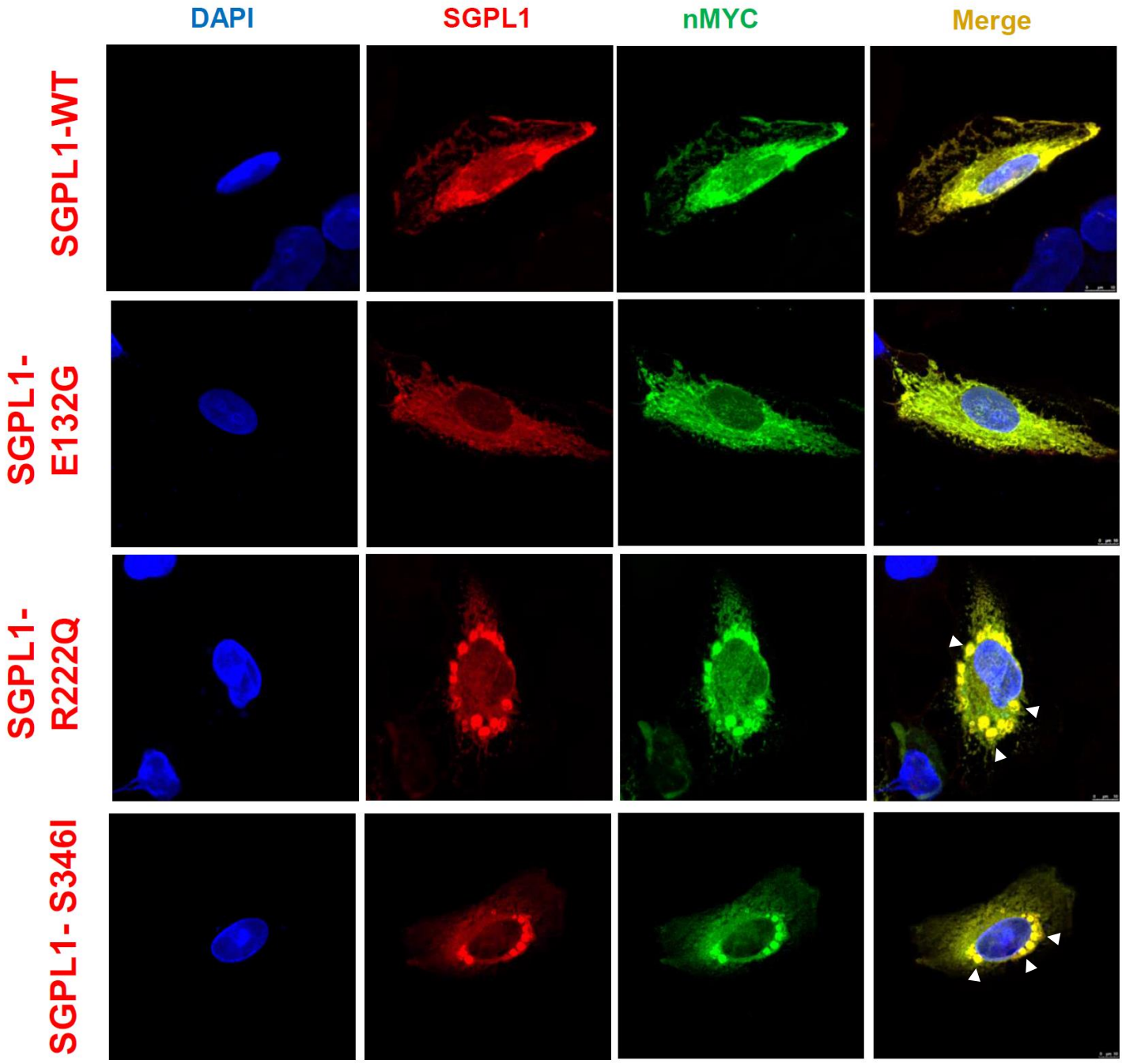

Supplemental Figure 6. Immunofluorescence of *SGPL1* cDNA clones representing wild type (WT) and mutant cDNA clones overexpressed in human immortalized undifferentiated podocytes. Podocytes were transfected with Myc-tagged wild-type (WT) and mutant clones of *SGPL1* detected in patients with nephrotic syndrome. Cells were fixed with cold acetone and coimmunostained with anti-SGPL1 (R&D Systems) (red) and anti-Myc antibody (green). Note that overexpressed p.R222Q and p.S346I variant proteins formed aggregates (white arrow heads) upon overexpression, whereas wild type and missense control p.E132G SGPL1 proteins did not show cellular aggregates.

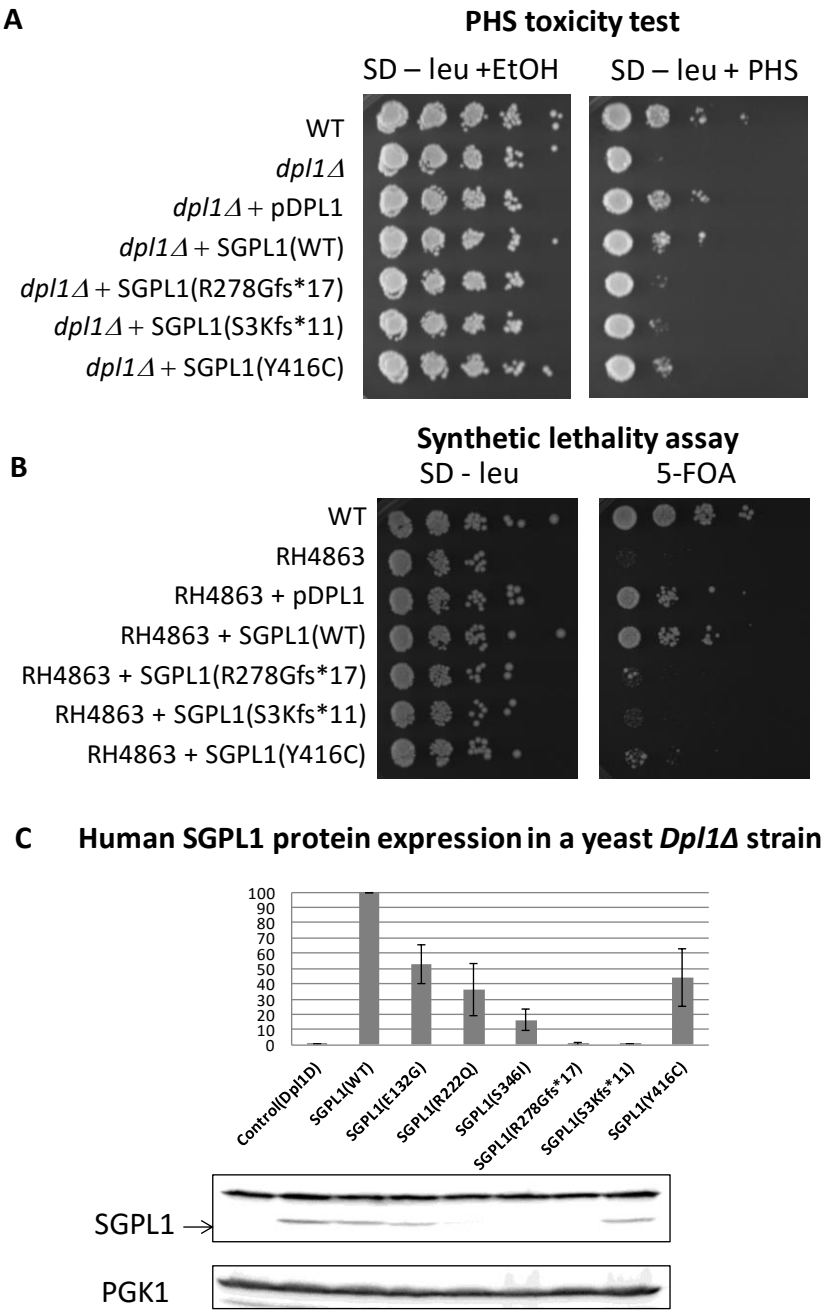

Supplemental Figure 7. Human *SGPL1* mutations fail to rescue yeast growth.
(A) Phytosphingosine toxicity test. Ability to complement *dpl1Δ* deletion on a medium containing phytosphingosine (PHS) was tested for human SGPL1 WT and the mutants Y416C, R278Gfs*17, S3Kfs*11. None of this mutants was able to restore the impaired growth of a dpl1 knockout strain.
(B) Synthetic lethality test. Synthetically lethal yeast strain RH4863, in which *DPL1* and *LCB3* were deleted, was maintained by expressing *LCB3* from a *URA3*-plasmid. Human WT SGPL1 expressing RH4863 survived on 5-FoA plates, showing to be able to compensate for the loss of *LCB3* and to degrade long-chain bases. However, overexpression of the mutants Y416C, R278Gfs*17, S3Kfs*11, observed in patients with NPHS type 14, did not allow for survival of *DPL1* (*SGPL1*) deficient strains.
(C) Human SGPL1 WT and mutants expression in a yeast *Dpl1Δ* strain. Protein expression of SGPL1 WT and mutants Glu132Gly, Arg222Gln, Ser346Ile, Arg278Glyfs*17, Ser3Lysfs*11, and Tyr416Cys in yeast Dpl1Δ strain. PGK1 was used as a loading control. Values correspond to 3 independent experiments and are shown as % to WT.

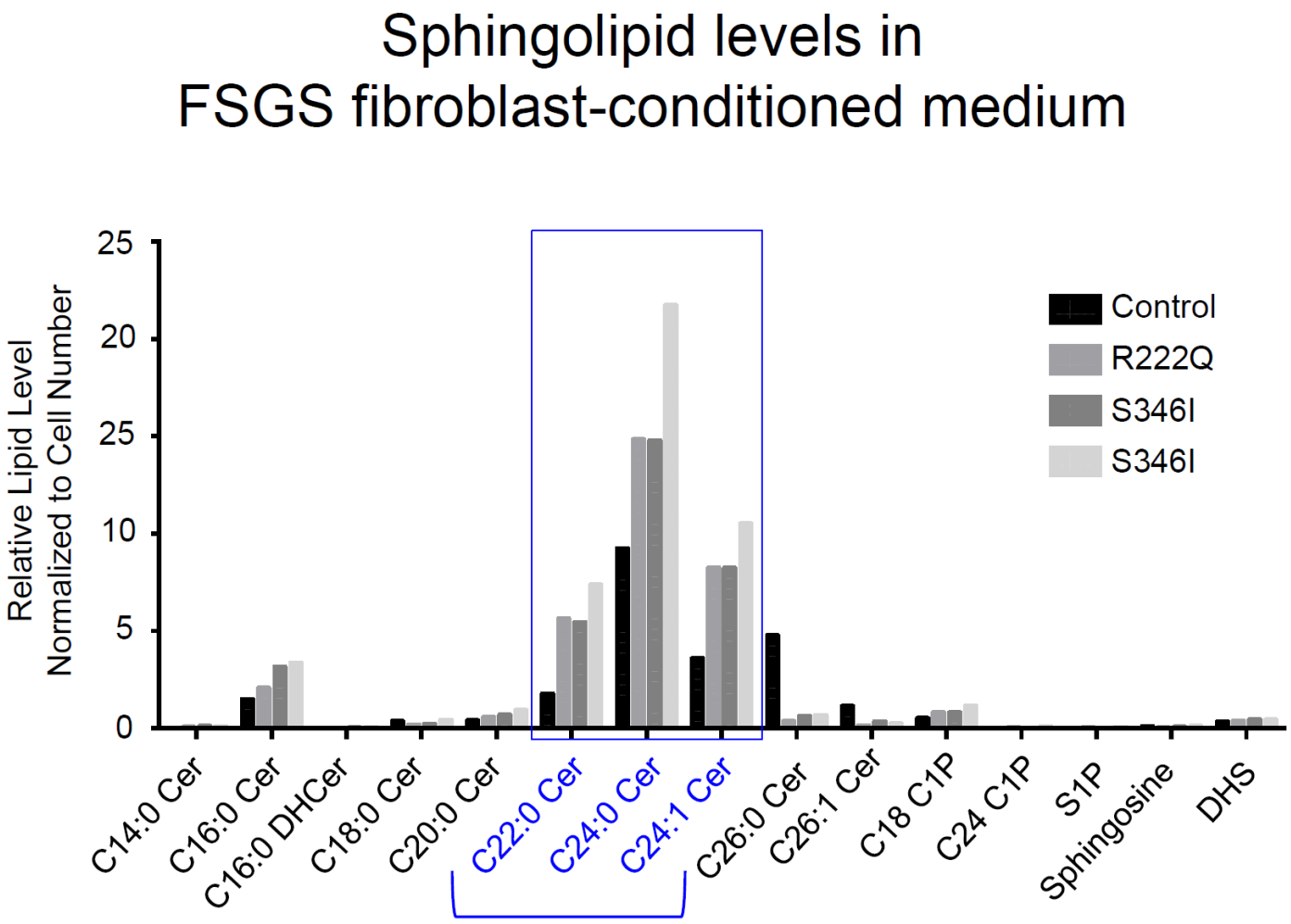

Supplemental Figure 8. Sphingolipid levels in fibroblast-conditioned medium. Sphingolipids were extracted from control and patient fibroblast-conditioned medium after 24h conditioning and analyzed by LC/MS, as described in Methods.

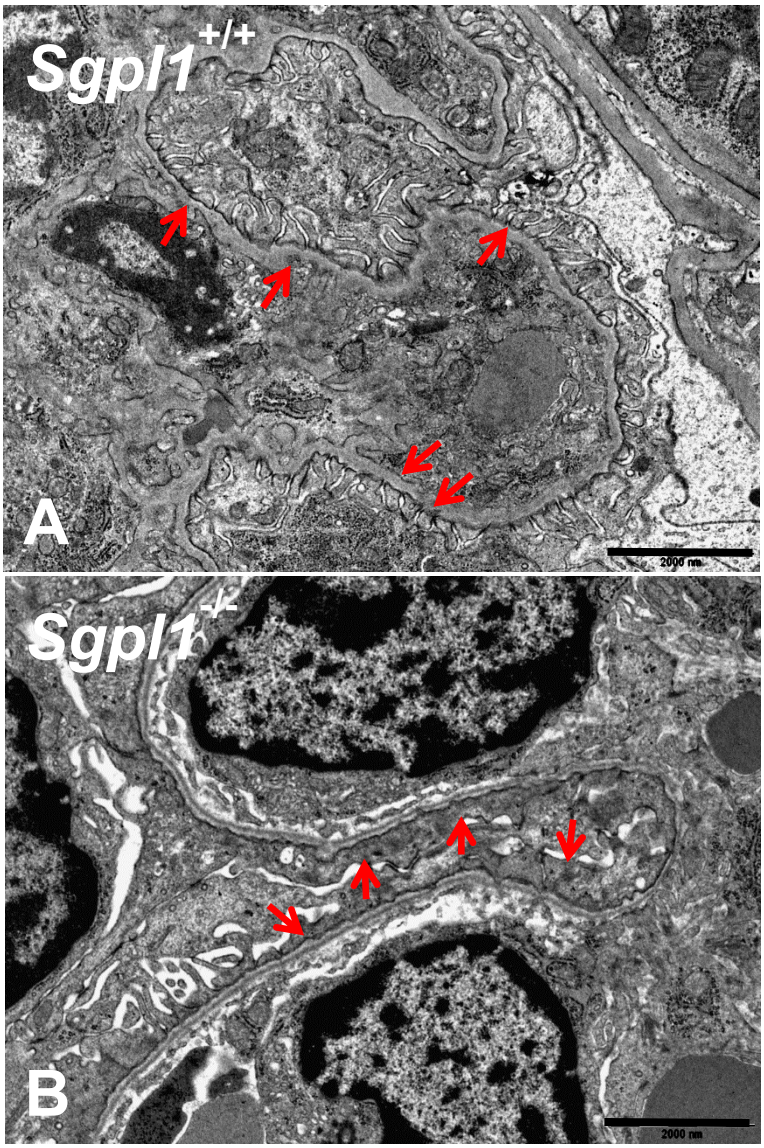

Supplemental Figure 9. Loss of *Sgpl1* causes foot process effacement.

Kidneys of 13 day old *Sgpl1*$^{+/+}$ and *Sgpl1*$^{-/-}$ mice were collected and renal morphology was examined by transmission electron microscopy (TEM).

(**A**) Podocyte foot processes (red arrows) are regularly spaced in kidneys of *Sgpl1*$^{+/+}$ mice.

(**B**) *Sgpl1*$^{-/-}$ kidneys exhibit complete foot process effacement (red arrows) and absence of slit-diaphragms. Scale bars are 2 μm.

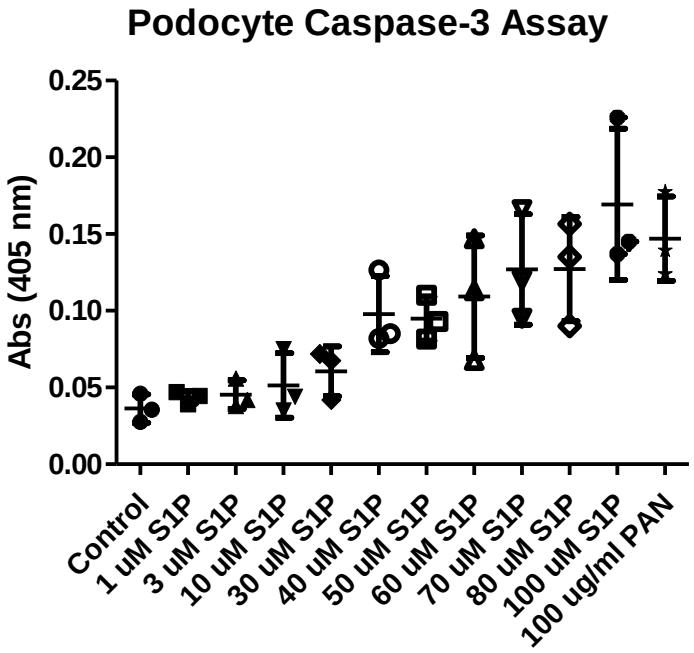

Supplemental Figure 10. Effect of sphingosine-1-phosphate (S1P) on apoptosis of cultured human podoyctes. S1P or puromycin aminonucleoside (PAN) was incubated for 24 hours and apoptosis was measured by caspase-3 assay. More than 40 μM of S1P induced significant apoptosis in cultured human podocytes. Data represent the mean ± standard deviation of three independent experiments.

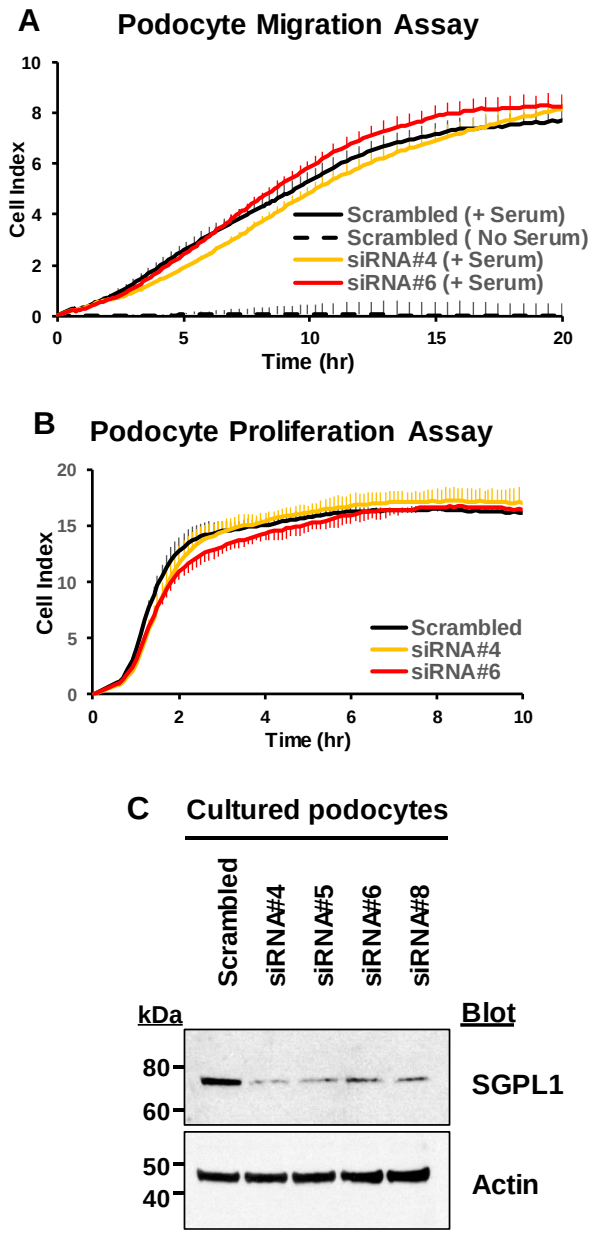

Supplemental Figure 11. Effects of *SGPL1* knockdown on migration and proliferation of cultured human podocytes.
(A) *SGPL1* knockdown using two different siRNAs did not have any effect on migration in undifferentiated cultured human podocytes.
(B) *SGPL1* knockdown did not affect proliferation of culture podocytes. Error bars in **A** and **B** are shown in one direction only for clarity and indicate SDs for 3 indipendent expreiments.
(C) The efficiency of *SGPL1* knockdown by 4 different siRNAs was confirmed by immunoblotting. Immunoblot is representative of 3 experiments.

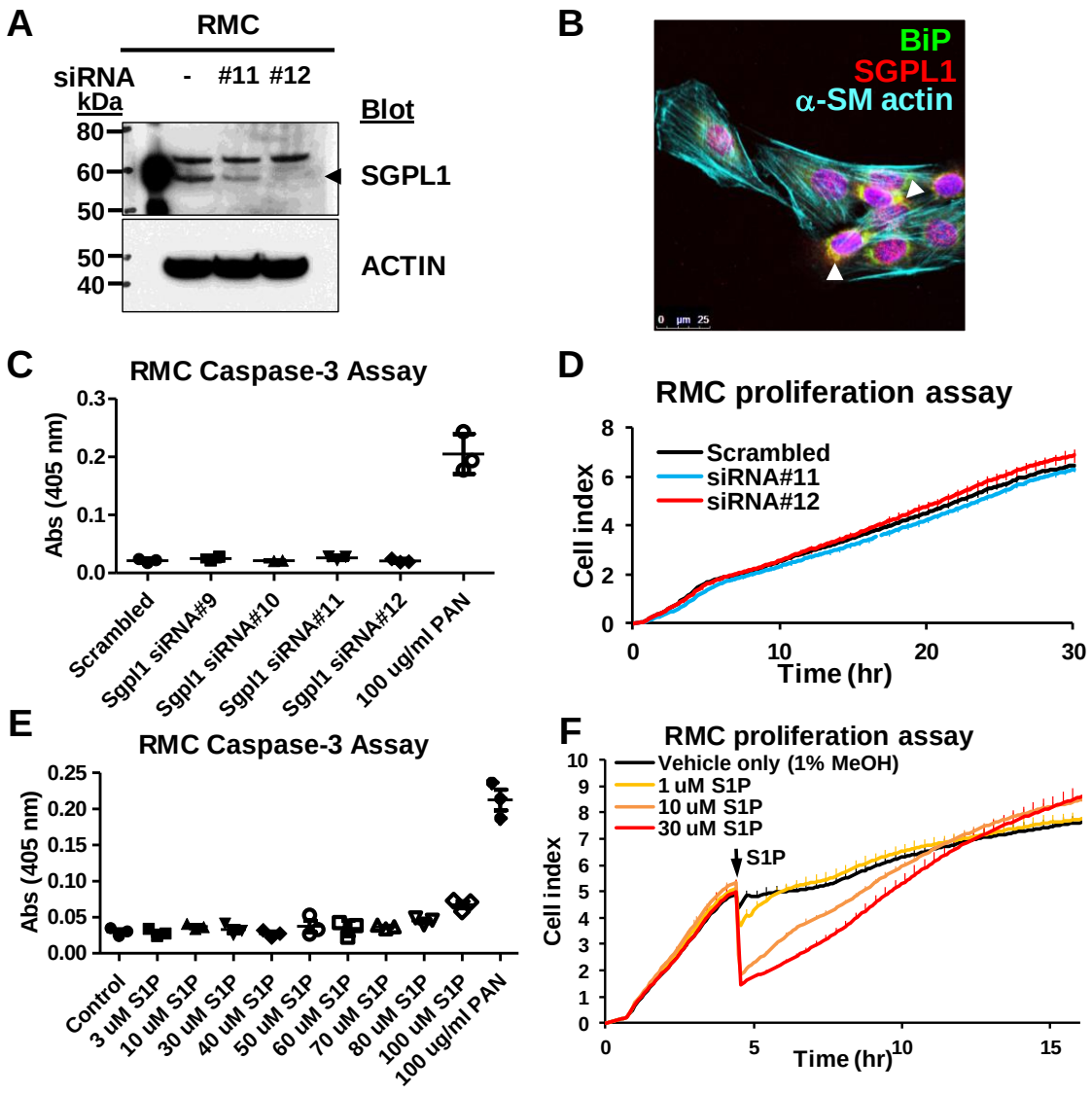

Supplemental Figure 12. Effects of *Sgpl1* knockdown and S1P administration on rat renal glomerular mesangial cells (RMCs).

(A) *Sgpl1* knockdown by siRNAs (siRNA#11 and siRNA#12) in RMCs significantly reduced SGPL1 protein. Immunoblot is representative of 3 experiments.

(B) Immunofluorescence of SGPL1 in RMCs. BiP (green), SGPL1 (red), and α-smooth muscle (SM) actin (sky blue).

(C) Knockdown of *Sgpl1* in RMCs did not induce apoptosis as measured by caspase-3 assay. D PAN, puromycin aminonucleoside.

(D) Knockdown of *Sgpl1* in RMCs did not affect cell proliferation rate using the xCELLigence system.

(E-F) Effect of sphingosine-1-phosphate (S1P) on apoptosis (**E**) or proliferation rate (**F**) of RMCs.

(E) Sphingosine-1-phosphate (S1P) administration did not significantly induce apoptosis in RMCs up to 100 μM. S1P or PAN was incubated for 24 hrs. Data represent the mean ± standard deviation of three independent experiments in **C** and **E**.

(F) S1P did not induce defects in proliferation of RMCs even though there was a transient drop in cell index with recovery upon addition of high concentration (≥ 10 μM) of S1P. Each cell index value corresponds to the average of more than triplicates in **D** and **F**.

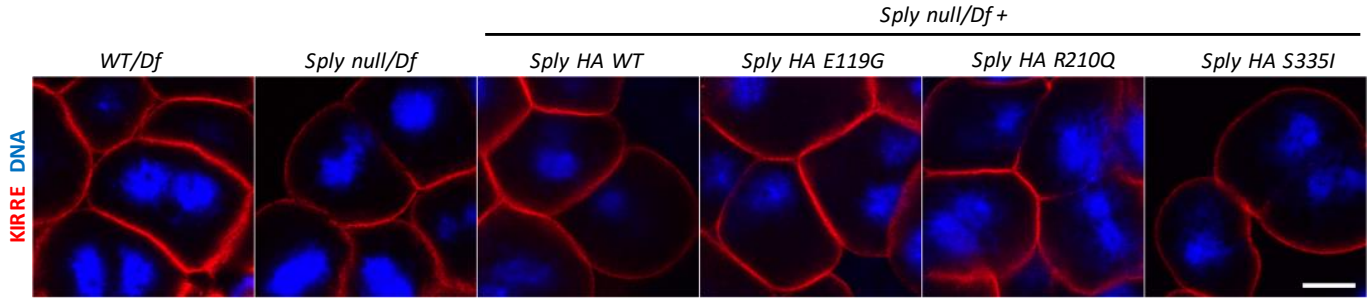

Supplemental Figure 13. *Sply* null hemizygous nephrocytes and SGPL1 mutations do not have any obvious impact on *Kirre* (*Neph1*) expression in nephrocytes.
Immunofluorescence of 3rd instar Garland nephrocytes, stained for the Neph1 ortholog, Kirre (red). No major changes on Kirre staining were observed in the different mutants. n=2 independent experiments (≥5 larvae per genotype). Nuclei were labeled with Hoechst (blue). Scale bar, 10 μm.

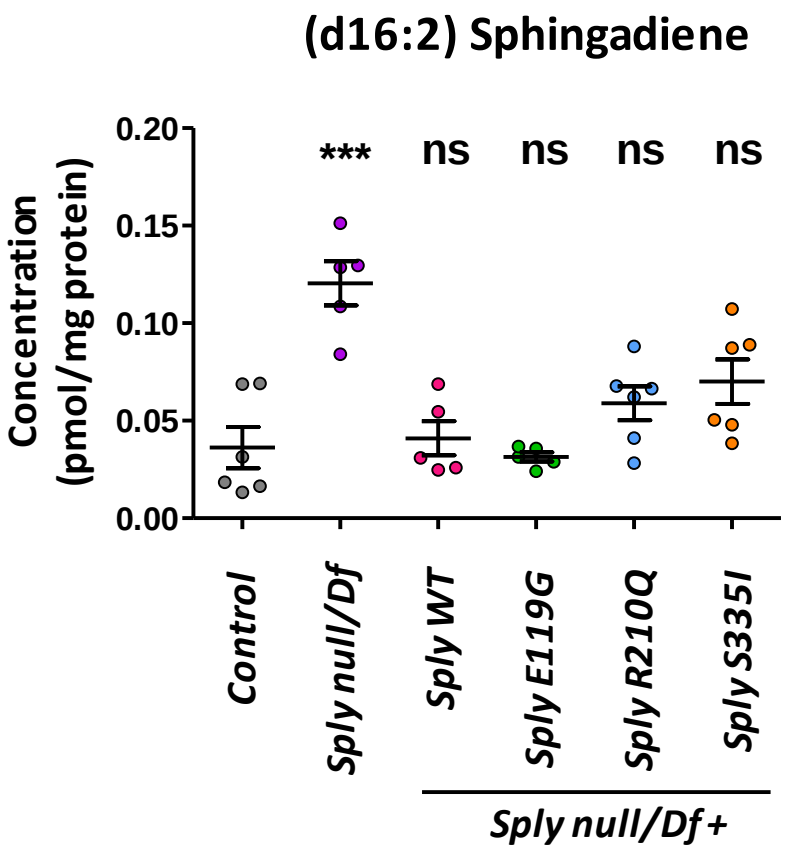

Supplemental Figure. 14. Accumulation of sphingadienes (SD) in *Sply null hemizygous* flies. *Sply null* hemizygous flies accumulate sphingadienes and this is rescued by *Sply* WT and E119G mutants. There is a trend towards accumulation of sphingadienes in the mutants R210Q and S335I, although this does not reach statistical significance. *Whole 3rd instar* larvae were collected and processed for LC/MS. (n= 6 independent experiments; for *Sply* null, *Sply* WT and *Sply* E119G, one analysis per group was removed due to poor quality of the chromatography). Control corresponds to WT larvae. Asterisks denote groups that are statistically different from control identified by one-way Analysis of Variance analysis. ***, $p<0.0005$; ns, not significant.

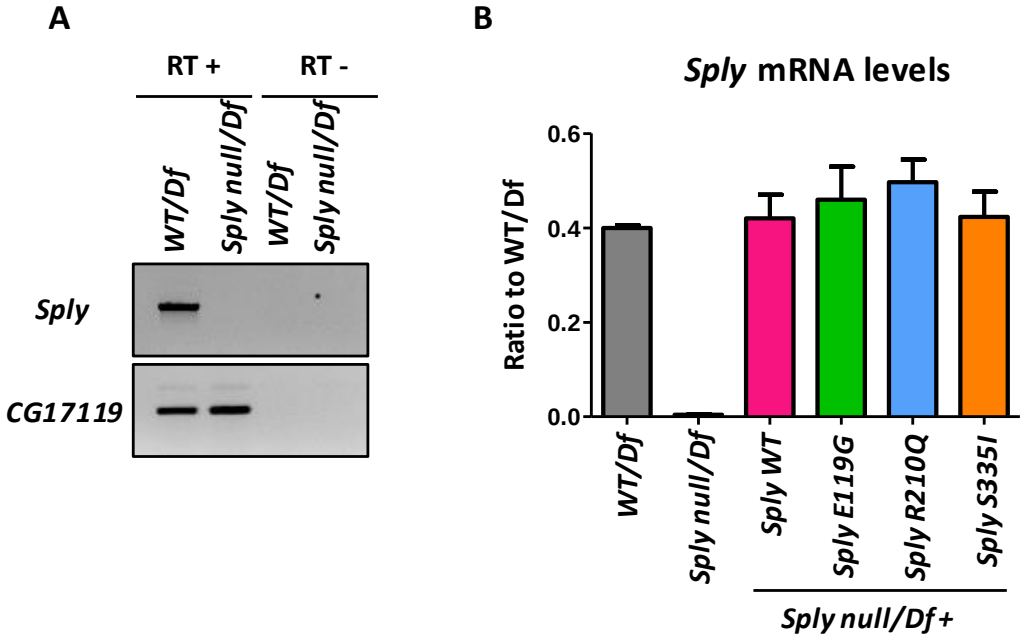

Supplemental Figure 15. *Sply* mRNA levels in *Drosophila*.

(A) *Sply* RT-PCR of 3rd instar larvae heterozygous for the *Df(2R)BSC433* (control) or *Sply null* hemizygous. Note the absence of *Sply* cDNA in *Sply null* hemizygous flies. CG1719 transcript was amplified as a control. n=2 independent experiments.

(B) *Sply* mRNA levels are not different between the *Sply* WT and the mutant rescue constructs. *Sply* qPCR of 3rd instar larvae heterozygous for the *Df(2R)BSC433* (control), *Sply null* hemizygous, or the rescue animals carrying the Sply transgenes WT, E119G, R210Q or S335I on the *Sply null* hemizygous background. n=3 independent experiments.